DOI: 10.1002/chem.200501330

Site-Selective Formation of Optically Active Inclusion Complexes of Alkoxo-Subphthalocyanines with β-Cyclodextrin at the Toluene/Water Interface

Kenta Adachi and Hitoshi Watarai*[a]

Abstract: Several subphthalocyanine derivatives that contain an alkoxo substituent as an axial ligand (RO-Subpc, R = 9-anthracenemethyl, benzyl, phenyl, 3,5-dimethylbenzyl, 3,5-dimethylphenyl, 4-methylbenzyl, and 4-methylphenyl) were synthesized. The formation of inclusion complexes of RO-Subpc with β-CD in DMSO and at the toluene/water interface was investigated by UV/Vis absorption spectroscopy, induced circular dichroism (ICD), and nuclear magnetic resonance (NMR) measurements. Interfacial tension measurements suggested that β-CD adsorbed as a monolayer at the toluene/water interface and probably orientated towards the toluene phase with its primary face. The 1:1 composition of β-CD·RO-Subpc inclusion complexes was confirmed in DMSO and at the toluene/water interface for BzO-Subpc, PhO-Subpc, MeBzO-Subpc, and MePhO-Subpc. A 2:1 inclusion complex of AnO-Subpc formed in DMSO. The observed ICD spectra of β-CD·RO-Subpc inclusion complexes are discussed with respect to molecular modeling and the simulation based on Tinoco–Kirkwood theory. Interestingly, the ICD spectra of β-CD·BzO-Subpc and β-CD·MeBzO-Subpc inclusion complexes exhibited a negative sign in DMSO and a positive sign at the toluene/water interface. This reversal of the ICD sign strongly suggests a difference in the structure of the inclusion complexes: β-CD at the interface formed the inclusion complex with its primary face, whereas the secondary face of β-CD bound favorably to RO-Subpc in DMSO.

Keywords: circular dichroism · cyclodextrins · inclusion complexes · liquid/liquid interface · subphthalocyanines

Introduction

Cyclodextrins (CDs) are cyclic oligosaccharides commonly consisting of six, seven, or eight α-D-glucopyranose units bound by α(1–4) linkages that are named α-, β-, and γ-cyclodextrin, respectively. In particular, β-cyclodextrin (β-CD) has an internal cavity shaped like a bottomless bucket of about 8 Å in depth and 6.0–6.5 Å in diameter (the smaller value is for the end with the primary hydroxy group (primary face) and the larger is for the end with the secondary hydroxy group (secondary face)),[1–3] as shown in Scheme 1. This cavity has a relatively low polarity and thus allows the accommodation of organic guest molecules. For this reason, CDs and their derivatives have been employed for fundamental studies in various fields, such as analytical chemistry,[4] synthetic chemistry,[5–8] and supramolecular science[9,10] as well as for application development in pharmaceutical technology, in which they are used in artificial enzymatic reactions,[11] molecular recognition,[12] chiral separation,[13] photodynamic therapy,[14] and drug delivery.[15,16] Despite all this research, the inclusion phenomena of CDs at the liquid/liquid interface have received little attention to date.

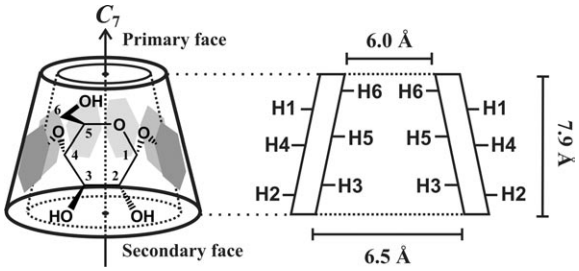

Scheme 1. Schematic representation of the shape of the β-cyclodextrin molecule with its cross-section on the right.

[a] K. Adachi, Prof. Dr. H. Watarai
Department of Chemistry, Graduate School of Science
Osaka University
Toyonaka, Osaka 560–0043 (Japan)
Fax: (+81) 6-6850-5411
E-mail: watarai@chem.sci.osaka-u.ac.jp

Supporting information (absorption spectra, curve fitting, ^{1}H NMR results in [D$_6$]DMSO, molecular modeling) for this article is available on the WWW under http://www.chemeurj.org/ or from the author.

In the past decade, we have investigated the adsorption and aggregation behavior of some dye molecules and metal complexes in the liquid/liquid system by means of various techniques.[17] The liquid/liquid interface that forms between two immiscible liquids is promising as a novel reaction field because the interface is a two-dimensional liquid with a thickness of a few nanometers.[18,19] This interface has some specific functions that are not found in the bulk phases, such as orientational adsorption, two-dimensional concentration, and interfacial aggregation.[20,21] Molecular self-organization and site-selective orientation at the liquid/liquid interface are predominant motifs in the application of interfacial phenomena for novel material design, biological systems, as well as their related science and technology. For instance, as dye molecules could be aligned as aggregates at the liquid/liquid interface, they may be used as nanometer-sized molecular devices in which transition dipoles are oriented in one direction. Moreover, it has been generally recognized that the interfacial orientation of proteins at the cell membrane governs functions such as molecular recognition and energy or information transfer on or through the membranes.[22] Therefore, the understanding of the mechanisms of interfacial adsorption and the inclusion reaction of CDs is very important for the development of material and life sciences.

Subphthalocyanine (Subpc) is a macrocycle formed by three coupled isoindole moieties that have a delocalized 14-π-electron system and an axial ligand coordinated to the central boron atom.[23,24] Recently, Subpcs have received considerable attention because they are excellent building blocks for the synthesis of asymmetric phthalocyanines[25] and useful materials for crystalline liquid[26,27] and nonlinear optics.[27–30] Native Subpc has a high molar absorptivity ($\varepsilon >$ 50000) and a halogen atom bound to the central boron atom, which is exchangeable with other nucleophiles. We have synthesized several novel subphthalocyanine derivatives with an alkoxo substitute at the axial position (RO-Subpc; see Scheme 2) as candidate guest molecules for β-CD.

In this study, the formation of inclusion complexes and the orientation behavior of RO-Subpc with β-CD were investigated in DMSO and at the toluene/water interface. Induced circular dichroism (ICD) spectra of the inclusion complexes were interpreted within the framework of the Tinoco–Kirkwood theory,[31,32] and the molecular modeling calculation was used to assess the structures of β-CD·RO-Subpc inclusion complexes in both systems. Experimental results have revealed for the first time that the inclusion site of β-CD for RO-Subpc is completely different at the liquid/liquid interface than in the bulk solution.

Results and Discussion

Spectral characterization of RO-Subpc compounds: The axially alkoxo-substituted subphthalocyanines were synthesized by the condensation of Cl-Subpc and the appropriate alcohol (Scheme 2), by using the procedure developed by Claessens et al.[33] with a slightly modified purification process. The formation of alkoxo-subphthalocyanine was monitored by the appearance of a new peak in the IR spectra at $\approx$1370 cm^{-1}, which was tentatively assigned to the stretching vibration of B–O bonds in RO-Subpc.[34]

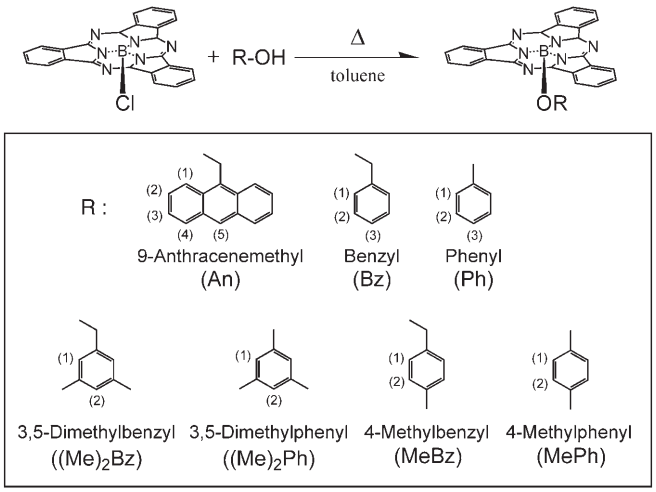

Scheme 2. Syntheses of subphthalocyanine derivatives with the alkoxo substituent in the axial position.

RO-Subpc compounds were highly soluble in dichloromethane, chloroform, toluene, dimethyl sulfoxide (DMSO), tetrahydrofuran (THF), acetone, and pyridine, and slightly soluble even in methanol and ethanol, but were insoluble in acetonitrile. In addition, they were stable in those solvents, except for aged DMSO and THF, in which they were bleached after 1 h. Similar to the original Cl-Subpc, RO-Subpc displays absorption bands in the UV (Soret band) and visible (Q band) regions (Figure 1 and Figure S1 in the Supporting Information). In the case of AnO-Subpc (Fig-

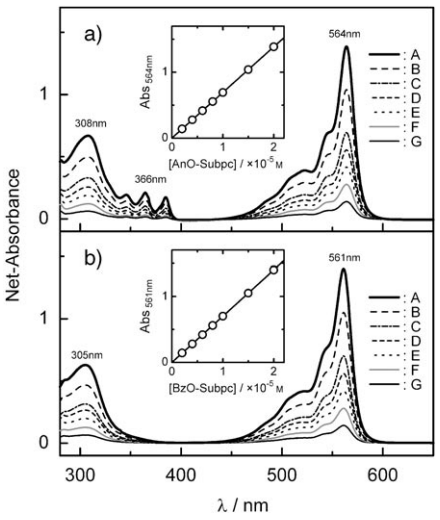

Figure 1. Absorption spectra of a) AnO-Subpc and b) BzO-Subpc in toluene at different concentrations: A) 2.0×10^{-5} M, B) 1.5×10^{-5} M, C) 1.0×10^{-5} M, D) 8.0×10^{-6} M, E) 6.0×10^{-6} M, F) 4.0×10^{-6} M, G) 2.0×10^{-6} M.

ure 1a), a new band between the Soret and the Q bands appears at about 330–400 nm. This smaller absorption band is assigned to the ^1L_a band of the anthracene moiety according to Platt's nomenclature.[35] Lambert–Beer plots for solutions of AnO-Subpc and BzO-Subpc in toluene are linear over at least 3 orders of magnitude in concentration (inset of Figure 1), which rules out any aggregation in toluene. This behavior is strikingly different from that of planner unsubstituted phthalocyanines, which show a high tendency to form aggregates by π–π stacking.

Formation of an inclusion complex between β-CD and RO-Subpc in DMSO: Typical examples are given in Figure 2, which shows the sectional absorption and induced circular dichroism (ICD) spectra of RO-Subpc in DMSO containing various concentrations of β-CD. When β-CD was added to BzO-Subpc solution, the Q band was shifted to a longer wavelength, accompanied by the appearance of an isosbestic point at 563 nm (Figure 2b). Other β-CD·RO-Subpc systems showed similar spectral changes, (see the Supporting Information) except for the β-CD·AnO-Subpc system. AnO-Subpc exhibited a spectral change in the ^1L_a band region upon addition of β-CD, whereas the Q band did not shift significantly (Figure 2a).

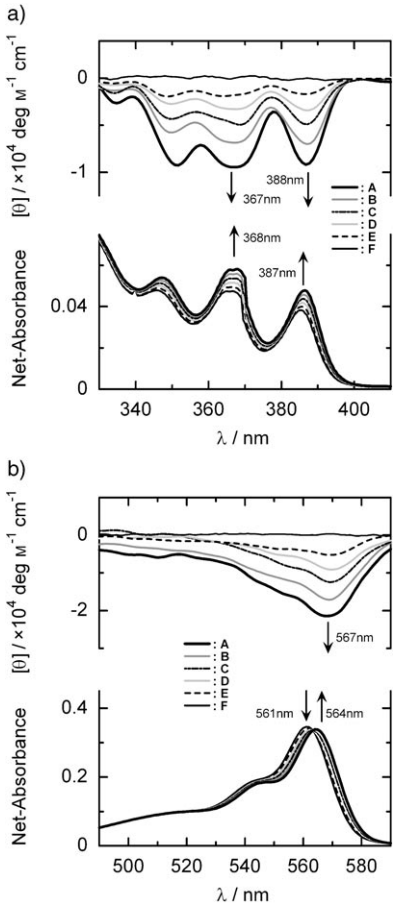

Figure 2. Induced circular dichroism (top) and absorption (bottom) spectra of a) AnO-Subpc and b) BzO-Subpc in DMSO at different concentrations of β-CD: A) 5.0×10^{-4} M, B) 3.0×10^{-4} M, C) 2.0×10^{-4} M, D) 1.5×10^{-4} M, E) 1.0×10^{-4} M, F) in the absence of β-CD. [RO-Subpc] = 5.0×10^{-6} M.

RO-Subpc compounds are inherently achiral and hence no circular dichroism bands were observed in DMSO in the absence of β-CD. In the presence of β-CD; however, BzO-Subpc displayed a negative ICD spectrum in the Q band region with the increase of β-CD concentration (Figure 2b). In the case of AnO-Subpc also, a negative band with some peaks was observed in the ^1L_a band region, although no ICD signals were shown around the Q band (Figure 2a). Other RO-Subpc compounds showed similar circular dichroism spectra with BzO-Subpc (see the Supporting Information). The conformation of the β-CD·RO-Subpc inclusion complex in DMSO will be discussed below on the basis of these ICD spectral results.

All observed changes in the absorption and circular dichroism spectra indicated the formation of an inclusion complex of β-CD with RO-Subpc in DMSO.[36] Inclusion of the SubPc skeleton into β-CD is impossible because it is much larger than the size of the β-CD cavity. Inclusion of the alkoxo-substituent moiety, therefore, seems more reasonable. To confirm the inclusion of an alkoxo group, we performed ^{1}H NMR measurements in the absence and presence of β-CD. Observed ^{1}H NMR spectral data in [D_6]DMSO are listed in Table S1 in the Supporting Information. The chemical shift of interior protons H3 and H5 of β-CD moved upfield by $\Delta\delta\sim0.009$ ppm. In contrast to this feature, no change was observed in the chemical shift of the proton H6, which is located near the rim of the primary face. Furthermore, although the Subpc skeleton protons were independent of the presence of β-CD, the alkoxo-substituent protons of RO-Subpc also shifted upfield ($\Delta\delta\sim$ 0.010 ppm). ^{1}H NMR signals of aromatic molecules are usually shifted upfield on inclusion in the cavity of CD.[37] Therefore, the present results clearly indicated that the alkoxo substituent was included in the β-CD cavity from the secondary face, whereas the Subpc skeleton was exposed to DMSO. Moreover, a comparison between the signals of the *ortho* proton of the alkoxo substituent in the absence and in the presence of β-CD (except for AnO-Subpc) showed that chemical shift changes in $(Me)_2$PhO-Subpc and $(Me)_2$BzO-Subpc were negligibly small compared to those of other RO-Subpc compounds. This indicated that the $(Me)_2$PhO and $(Me)_2$BzO moieties were inserted less deeply into the β-CD cavity than BzO, PhO, MeBzO, and MePhO groups.[38]

Stability constant of β-CD·RO-Subpc inclusion complex in DMSO: The formation of a 1:1 inclusion complex between β-CD and aromatic compounds has been extensively reported.[1–3,39–45] Assuming the formation of a 1:1 β-CD·RO-Subpc inclusion complex in the present systems also [Eq. (1)], we analyzed the observed ICD spectral data by means of a Benesi–Hildebrand-type equation [Eq. (2)]:[46]

$$\beta\text{-CD} + \text{RO-Subpc} \overset{K_{stb,1}}{\rightleftarrows} \beta\text{-CD}\cdot\text{RO-Subpc} \quad (1)$$

$$\frac{1}{I-I_0} = \frac{1}{A} + \frac{1}{AK_{stb,1}[\beta\text{-CD}]} \quad (2)$$

where $K_{stb,1}$ is the stability constant for the formation of the 1:1 β-CD·RO-Subpc inclusion complex and the constant is defined as $A = \Delta[\theta][\text{RO-Subpc}]$, in which $\Delta[\theta]$ and [RO-Subpc] are, respectively, the change in the molar ellipticity between the free and complexed RO-Subpc and the initial concentration of RO-Subpc. I and I_0 stand for maximum circular dichroism intensities in the presence and absence of β-CD, respectively, and [β-CD] is the initial concentration of β-CD. Equation (2) holds under the experimental conditions of a higher concentration of β-CD than that of RO-Subpc (at least 10 times). In the case of BzO-Subpc, the plot of $1/(I-I_0)$ versus 1/[β-CD] gave a straight line (Figure 3b), indicating the formation of 1:1 inclusion complexes of β-CD·BzO-Subpc. The $K_{stb,1}$ values were taken as the intercept on the y axis. The 1:1 stoichiometric analysis was applicable to all RO-Subpc systems, except for the AnO-Subpc system.

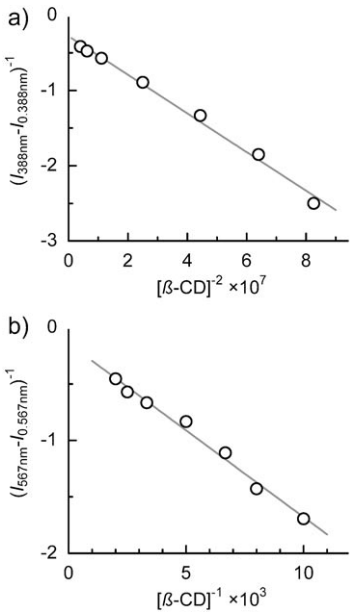

Figure 3. Benesi–Hildebrand plots for a) β-CD·AnO-Subpc and b) β-CD·BzO-Subpc inclusion complex in DMSO. The solid line is the best fit of the data to Equation (2) or (4). [RO-Subpc] = 5.0×10^{-6} M.

As for the β-CD·AnO-Subpc system, the plot according to Equation (2) did not afford a straight line (not shown). Therefore, the formation of the 2:1 β-CD·AnO-Subpc inclusion complex [Eq. (3)] was postulated and the spectral data was analyzed with Equation (4):

$$2\,\beta\text{-CD} + \text{RO-Subpc} \xrightarrow{K_{stb,2}} (\beta\text{-CD})_2 \cdot \text{RO-Subpc} \quad (3)$$

$$\frac{1}{I-I_0} = \frac{1}{A} + \frac{1}{AK_{stb,2}[\beta\text{-CD}]^2} \quad (4)$$

where $K_{stb,2}$ is the stability constant for the formation of a 2:1 β-CD·RO-Subpc inclusion complex. Figure 3a exhibits plots of $1/(I-I_0)$ against $1/[\beta\text{-CD}]^2$ for AnO-Subpc solution containing β-CD. This plot shows a good linearity, indicating that the β-CD·AnO-Subpc inclusion complex has mainly a 2:1 stoichiometry in this system. The values of $K_{stb,n}$ for all β-CD·RO-Subpc systems examined are summarized in Table 1. Moreover, we also obtained $K_{stb,n}$ values from the UV/Vis absorbance change. In the cases of $(Me)_2$BzO-Subpc and $(Me)_2$PhO-Subpc, the stability constant, $K_{stb,1}$, could not be obtained because the spectrum-shift upon addition of β-CD was too small. The $K_{stb,n}$ values obtained spectrophotometrically are almost equal to those evaluated from the induced CD intensity changes. However, the reliability of $K_{stb,n}$ values was better for those obtained from the CD intensity than those obtained from the change in the UV/Vis absorbance because the absorbance change was smaller than the CD intensity change.

The stability constants between β-CD and various alkyl benzene compounds have been reported in which the decreasing order of *p*-xylene > toluene > 1,3,5-trimethylbenzene was found.[47] This is in good agreement with the present results for MeBzO-Subpc and MePhO-Subpc, containing an aromatic ring with a methyl group in the *para*-position, that showed large stability constants with β-CD molecule which decreased in the order MeBzO-Subpc > BzO-Subpc > $(Me)_2$BzO-Subpc and MePhO-Subpc > PhO-Subpc > $(Me)_2$PhO-Subpc. From these results, it is concluded that one methyl group in the *para* position of alkoxo substituents can stabilize the inclusion complex with β-CD molecule, while two methyl groups in the *meta* positions interferred with deep insertion of the axial RO substituent into the β-CD cavity from the secondary face side.

Table 1. Stability constants of β-CD·RO-Subpc inclusion complexes in DMSO and at the toluene/water interface.

Compound	Host:Guest (in DMSO)	$K_{stb,1}$ [M^{-1}][a] UV/Vis	ICD	Host:Guest (at the interface)	$K'_{stb,1}$ [M^{-1}][b] HSS
AnO-Subpc	2:1	$(2.53\pm0.53)\times10^4$[c]	$(3.30\pm0.29)\times10^4$[c]	–	–
BzO-Subpc	1:1	$(1.57\pm0.63)\times10^3$	$(0.92\pm0.33)\times10^3$	1:1	$(3.24\pm0.13)\times10^5$
PhO-Subpc	1:1	$(1.20\pm0.55)\times10^3$	$(0.88\pm0.30)\times10^3$	1:1	$(2.01\pm0.43)\times10^5$
$(Me)_2$BzO-Subpc	1:1	–	$(0.40\pm0.11)\times10^3$	–	–
$(Me)_2$PhO-Subpc	1:1	–	$(0.31\pm0.09)\times10^3$	1:1	$(3.79\pm0.09)\times10^5$
MeBzO-Subpc	1:1	$(2.23\pm0.77)\times10^3$	$(1.83\pm0.19)\times10^3$	1:1	$(2.24\pm0.07)\times10^5$
MePhO-Subpc	1:1	$(1.85\pm0.63)\times10^3$	$(1.69\pm0.22)\times10^3$	–	–

[a] Stability constant of the β-CD·RO-Subpc inclusion complex. [b] Interfacial stability constant of the βCD·RO-Subpc inclusion complex. [c] $K_{stb,2}$ [M^{-2}].

Interfacial adsorption of β-CD at the toluene/water interface: The equilibrium interfacial tension, γ, in the toluene/water system was measured with various concentrations of β-CD in the aqueous phase, $[\beta\text{-CD}]_a$ (Figure 4). The relationship between γ and $[\beta\text{-CD}]_a$ is thus expressed by Equation (5),[48,49]

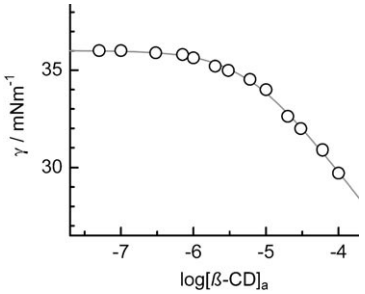

Figure 4. Lowering of interfacial tension owing to the adsorption of β-CD in the toluene/water system at 25 °C. The solid line is the best fit of the data to Equation (5).

$$\gamma = \gamma_0 - aRT \ln\left(1 + \frac{K'_{CD}[\beta\text{-CD}]_a}{a}\right) \quad (5)$$

where γ_0 is the interfacial tension in the absence of β-CD R is the gas constant, T is the absolute temperature, and a is the interfacial saturated concentration. Equation (6) gives K'_{CD}, the interfacial adsorption constant of β-CD:

$$K'_{CD} = \frac{[\beta\text{-CD}]_i}{[\beta\text{-CD}]_a} \quad (6)$$

$[\beta\text{-CD}]_i$ represents the interfacial concentration, and $[\beta\text{-CD}]_a$ is the aqueous concentration. The values for K'_{CD} and a in Equation (5) were obtained from Figure 4 as 8.27×10^{-4} dm and 8.54×10^{-9} mol dm^{-2}, respectively.

From the observed saturated interfacial concentration, the area per molecule for β-CD was calculated to be ≈190 Å^2. This area is almost equal to the vertical sectional area of the β-CD molecule against the C_7 axis (206 Å^2; incidentally, the cross-sectional area along the C_7 axis is estimated to be 155 Å^2). It is known that aromatic compounds such as benzene, toluene, and xylene are well imbedded in the β-CD cavity with little distortion of the macrocycle structure of β-CD.[50,51] Therefore, it was concluded that β-CD was adsorbed at the toluene/water interface to form the inclusion complex with a toluene molecule. Moreover, owing to the higher hydrophobicity of the primary face (the number of hydroxy groups on the primary face is 7, against 14 on the secondary face), the primary face of β-CD may be adsorbed at the toluene/water interface with the inclusion of a toluene molecule inside the cavity.

Induced circular dichroism of β-CD·RO-Subpc inclusion complexes at the toluene/water interface: The interfacial formation of the optically active complex of β-CD with RO-Subpc in the toluene/water system was directly observed by means of centrifugal liquid membrane-circular dichroism spectroscopy (CLM-CD),[52] in which CD spectroscopy is combined the CLM method to measure CD spectra of the interfacial species. The principle of the CLM technique was described elsewhere.[53] Figure 5 shows the ICD spectra of β-CD·RO-Subpc inclusion complexes at the toluene/water interface. Although ICD spectra are observed in the Q band region of the absorption spectra of RO-Subpc in toluene, their signs are different: mainly positive for BzO-Subpc and MeBzO-Subpc, but negative for PhO-Subpc and MePhO-Subpc. In the case of other RO-Subpc compounds, no ICD signal was observed in the toluene/water system. A particularly interesting result is that the negative ICD spectra for BzO-Subpc and MeBzO-Subpc in DMSO were reversed to positive ones at the toluene/water interface. This indicates that the configuration of β-CD·BzO-Subpc and β-CD·MeBzO-Subpc inclusion complexes in DMSO is different from those at the interface. To check the LD effect in this system, we also measured the LD spectra under the same sample conditions as for the CD measurement. However, there was no LD spectra in all cases, which led to the conclusion that the CD spectra of the β-CD·RO-Subpc inclusion complex molecules formed at the toluene/water interface did not include any LD contribution. This suggests their random orientation on the lateral plane of the interface. The structure of the β-CD·RO-Subpc inclusion complex at the toluene/water interface will be discussed below, along with that in DMSO.

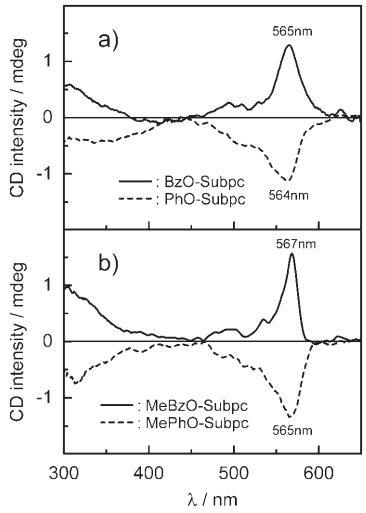

Figure 5. Inversion of the induced circular dichroism spectra of the interfacial β-CD inclusion complexes of RO-Subpc in the toluene/water system; a) BzO-Subpc (——) and PhO-Subpc (-----); b) MeBzO-Subpc (——) and MePhO-Subpc (-----). $[\beta\text{-CD}]_a = 1.0\times10^{-4}$ M. $[\text{RO-Subpc}]_o = 2.0\times10^{-5}$ M.

We also performed the batch distribution examination for the above four RO-Subpc compounds in the toluene/water system (see the Experimental Section), then measured the

CD spectra of the separated toluene and aqueous phases to check the solubility of β-CD·RO-Subpc inclusion complexes in the toluene and aqueous phases; they did not show any ICD signals. Therefore, it was confirmed that β-CD·RO-Subpc inclusion complexes were formed only at the toluene/water interface.

Because the concentrations of β-CD in the aqueous phase (Figure 5) are similar to that of RO-Subpc in the toluene phase, we could not estimate an interfacial stability constant, $K'_{cpx,n}$, and the stoichiometry of β-CD·RO-Subpc inclusion complexes formed at the toluene/water interface according to Equation (1) or (3). Thus, the composition ratio in β-CD·RO-Subpc complexes was analyzed by means of an ICD Job plot.[54] For this purpose, the maximum wavelength of the complexation-induced circular dichroism spectrum was plotted against the $[RO\text{-}Subpc]_o/\{[\beta\text{-}CD]_a+[RO\text{-}Subpc]_o\}$ concentration ratios, keeping the sum of the initial concentrations of β-CD and RO-Subpc constant ($=2.0\times10^{-5}$ M). As shown in Figure 6, the continuous variation plots revealed maxima at 0.5, indicating the formation of 1:1 complexes for all BzO-Subpc, PhO-Subpc, MeBzO-Subpc, and MePhO-Subpc systems. This stoichiometry was in good agreement with that observed in DMSO.

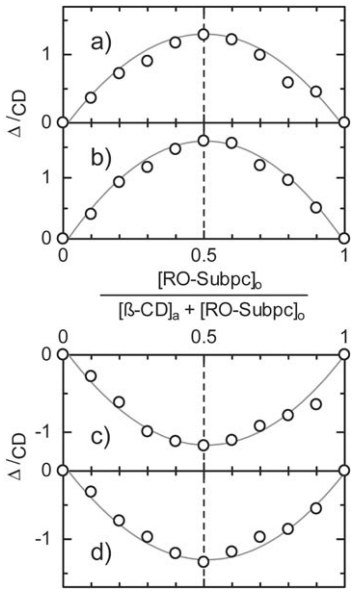

Figure 6. Job analysis of β-CD inclusion complex in the toluene/water system; a) BzO-Subpc, b) MeBzO-Subpc, c) PhO-Subpc, and d) MePhO-Subpc. The sum of the β-CD and RO-Subpc concentrations is 2.0×10^{-5} M.

Stability constant of β-CD·RO-Subpc inclusion complex at the toluene/water interface: The high-speed stirring (HSS) method[55] was used to determine the interfacial stability constant, K'_{stb}, of the β-CD·RO-Subpc inclusion complex. From HSS measurements in the absence of β-CD, it was confirmed that any RO-Subpc derivatives were not adsorbed at the toluene/water interface. On the other hand, in the presence of β-CD in the aqueous phase, the RO-Subpc concentration in the toluene phase was decreased by high-speed stirring (5000 rpm), which correctly indicated the formation of the β-CD·RO-Subpc inclusion complex at the toluene/water interface. The difference between the absorbances of the toluene phase under the high-speed (5000 rpm) and low-speed (200 rpm) stirring conditions, ΔA, and the absorbance of the bulk toluene phase, A_o, under high-speed stirring is expressed by Equations (7) and (8):

$$\Delta A = \varepsilon l[\beta\text{-CD}\cdot\text{RO-Subpc}]_i\frac{S_i}{V_o} \quad (7)$$

$$A_o = \varepsilon l[\text{RO-Subpc}]_o \quad (8)$$

where ε is the molar absorptivity of RO-Subpc in toluene, l is the optical path length of the flow cell (1.0 cm), S_i is the total interfacial area during stirring, V_o is the volume of the toluene phase, $[RO\text{-}Subpc]_o$ [M] is the concentration of RO-Subpc in the toluene phase, and $[\beta\text{-CD}\cdot RO\text{-}Subpc]_i$ [mol dm^{-2}] is the interfacial concentration of β-CD·RO-Subpc inclusion complex at the toluene/water interface. The total interfacial area, S_i, in the toluene/water system was already reported to be 2.0×10^2 dm^2.[56] The interfacial formation constant of the inclusion complex between RO-Subpc and β-CD at infinitely diluted concentration [Eq. (9)] is defined by Equation (10).

$$\beta\text{-CD}+\text{RO-Subpc}\overset{K'_{stb,1}}{\rightleftarrows}\beta\text{-CD}\cdot\text{RO-Subpc} \quad (9)$$

$$K'_{stb,1} = \frac{[\beta\text{-CD}\cdot\text{RO-Subpc}]_i}{[\beta\text{-CD}]_i[\text{RO-Subpc}]_o} \quad (10)$$

In the toluene/water system, the $[\beta\text{-CD}\cdot RO\text{-}Subpc]_i$ values of each RO-Subpc compound were determined by changing the concentration of $[RO\text{-}Subpc]_o$ and keeping the β-CD concentration fixed at 2.0×10^{-4} M. Only BzO-Subpc, MeBzO-Subpc, PhO-Subpc, and MePhO-Subpc showed the formation of an inclusion complex with β-CD at the interface (Figure 7). The observed plots showed saturation curves resembling a Langmuir adsorption isotherm. From Equations (6) and (10), and the Langmuir adsorption isotherm of β-CD, we obtain Equation (11) for the interfacial isotherm of β-CD·RO-Subpc inclusion complex.

$$[\beta\text{-CD}\cdot\text{RO-Subpc}]_i = \frac{aK_{CD}K_{stb,1}[\beta\text{-CD}]_a[\text{RO-Subpc}]_o}{(a+K'_{CD}[\beta\text{-CD}]_a)\{1+K'_{stb,1}[\text{RO-Subpc}]_o\}} \quad (11)$$

The interfacial stability constant, $K'_{stb,1}$, of the β-CD·RO-Subpc inclusion complex was determined by means of a nonlinear least-squares method according to Equation (11). The values of $K'_{stb,1}$ are also listed in Table 1. As can be seen from Table 1, the RO-Subpc with the methyl group at the *para* position of the alkoxo substituent afforded the higher interfacial stability constants; $K'_{stb,1}=(3.79\pm0.07)\times10^5$ M^{-1} for MeBzO-Subpc and $K'_{stb,1}=(2.24\pm0.09)\times10^5$ M^{-1} for MePhO-Subpc. This tendency was also observed in DMSO. The values of the stability constant at the toluene/water in-

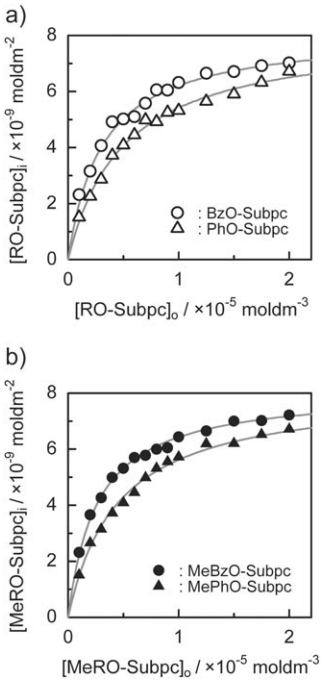

Figure 7. The interfacial equilibrium isotherm of β-CD·RO-Subpc inclusion complex measured by means of the HSS method in the toluene/water system. a) BzO-Subpc (○) and PhO-Subpc (△); b) MeBzO-Subpc (●) and MePhO-Subpc (▲). The solid line is the best fit of the data to Equation (11). $[\beta\text{-CD}]_a = 2.0\times10^{-4}$ M.

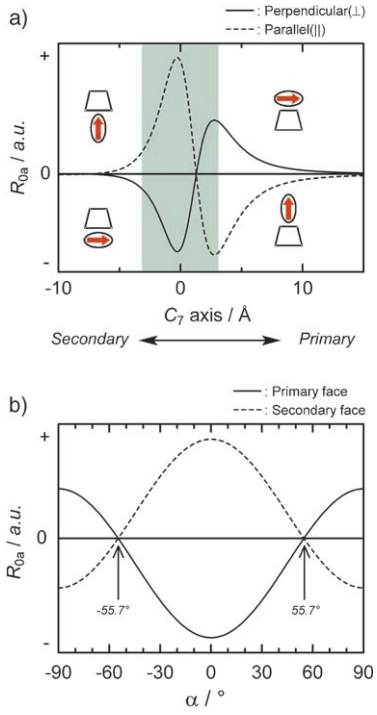

Figure 8. The dependence of calculated rotational strength, R_{0a}, of a β-CD·chromophore inclusion complex against a) the position and b) the orientation of the chromophore on the C_7 axis of β-CD. a) Solid and broken lines refer to the transition dipoles perpendicular (⊥) and parallel (||) to the C_7 axis, respectively. The gray zone represents the exclusion region in β-CD for Subpc (≈8 Å). b) Solid and broken lines refer to the position of the transition dipoles on the primary and secondary face, respectively.

terface were ≈30× larger than those in DMSO, indicating that the hydrophobic cavity of β-CD adsorbed at the toluene/water interface could strongly incorporate RO-Subpc compounds. More recently, Liu et al.[57] studied complexation between β-CD and various steroids. They concluded that the stability constant of the β-CD·steroid inclusion complex was enhanced by co-inclusion of an aromatic compound. Because the β-CD molecule adsorbed at the toluene/water interface is expected to include a toluene molecule, the stability enhancement observed in the present study suggested the favorable interaction between a co-included toluene molecule and a RO-Subpc in β-CD.

Structure of the β-CD·RO-Subpc inclusion complex in DMSO and at the toluene/water interface: Many ICD phenomena of cyclodextrin-chromophore inclusion complexes[58–62] have been analyzed with high accuracy on the basis of the Tinoco–Kirkwood coupled oscillator expression[31,32] [Eq. (12)] (see the Experimental Section). Equation (12) makes it possible to determine the orientation of the chromophore molecule incorporated in the cyclodextrin cavity from the sign of the ICD spectra of the inclusion complex. Figure 8 shows the dependence of the rotational strength of a chromophore, calculated with Equation (12), upon the position and orientation of the electric transition dipole on the C_7 axis of β-CD, in which the origin of the C_7 axis is the center of β-CD molecule. In the case of β-CD·RO-Subpc inclusion complexes, the alkoxo substituent of RO-Subpc is the only group incorporated into the β-CD cavity. Consequently, the transition dipole of the Subpc skeleton is always located outside this cavity. Subpc has two transition dipoles in the Q band, both in the same plane determined by three *meso*-nitrogen atoms.[63] As can be seen from Figure 8a, when the transition dipole of Subpc skeleton is in the parallel (||) or perpendicular (⊥) position with respect to the C_7 axis on the primary face, an observed ICD spectrum will give a negative or positive sign, respectively. Conversely, on the secondary face, it shows just the reversed situation. Additionally, the sign of ICD is reversed at $\alpha = 54.7°$, where α is the tilt angle defined between the transition dipole moment and the C_7 axis of β-CD (Figure 8b). It appears that the ICD sign is quite sensitive to the position and orientation of the transition dipole of the Subpc skeleton.

Some probable structures with minimum energies in that are consistent with the ICD spectral behavior of β-CD·RO-Subpc inclusion complexes in DMSO and at the toluene/water interface are shown in Figure 9. As can be seen, the main difference between the interactions with the primary and the secondary faces in the optimized structures is the value of the tilt angle (α) of the Subpc skeleton. For the inclusion of BzO-Subpc at either the primary or the secondary face of β-CD, the value of α is greater than 54.7° (Figure 9), but for the inclusion of PhO-Subpc, values of α are 33.5°

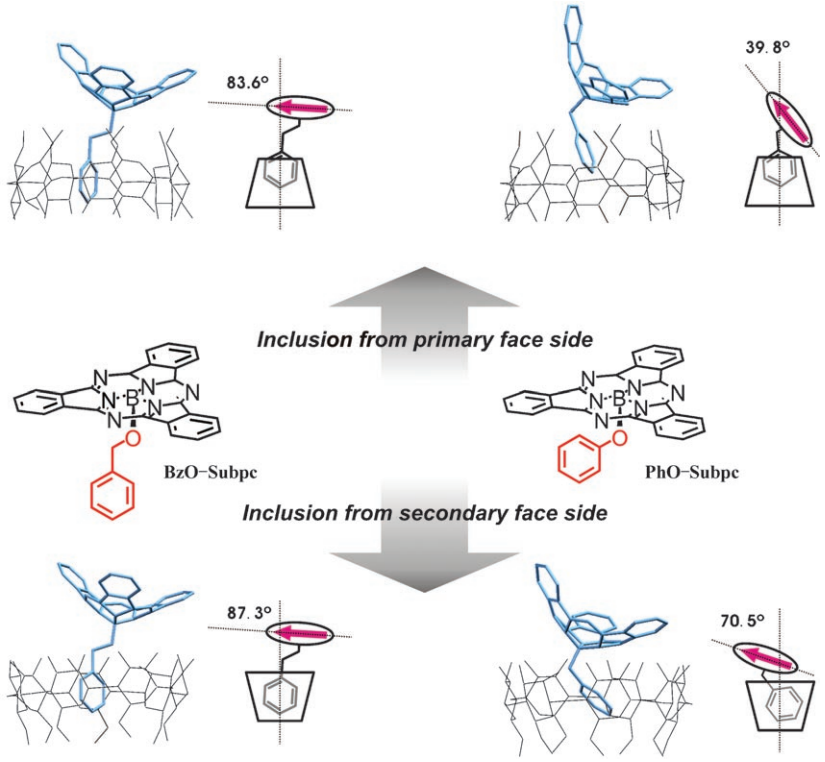

Figure 9. Estimated energy-minimized structures of β-CD·BzO-Subpc and β-CD·PhO-Subpc inclusion complexes from the primary face and secondary face. Hydrogen atoms are omitted for clarity.

and 70.5° for the primary and secondary faces, respectively. These results are attributable to the tighter embracing of the alkoxo substituent at the primary face (size: 6.0 Å) of β-CD than at the secondary face (6.5 Å). ICD signals of these optimized structures with minimum energies were estimated by comparing their tilt angles (α) with the coupled oscillator simulation according to the Tinoco–Kirkwood theory (Figure 8). The calculated ICD signals around the Q band of BzO-Subpc and PhO-Subpc bound with β-CD from the secondary face were both negative. These are in agreement with the observed ICD signals in DMSO, indicating a "lid-type" geometry for the inclusion complexes of BzO-Subpc and PhO-Subpc from the secondary face of β-CD.[64] The computed molecular structures indicated that BzO-Subpc and PhO-Subpc were probably entering the β-CD cavity from both the primary and the secondary faces. However, at the toluene/water interface, the alkoxo substituent of BzO-Subpc and PhO-Subpc may preferentially enter from the primary face side of β-CD to form the inclusion complex because the interfacial tension measurement in the toluene/water system suggested interfacial adsorption with the primary face of β-CD from the aqueous phase. The estimated ICD spectra from optimized structures showed that the signal in the Q band region of β-CD·BzO-Subpc and β-CD·PhO-Subpc inclusion complex with the primary face was positive and negative, respectively. This excellent agreement between the experimental ICD signals in the CLM-CD measurements and the estimated ones of the molecular modeling suggested that the BzO-Subpc and PhO-Subpc molecules were preferentially embraced by the primary face of β-CD adsorbed at the toluene/water interface.

The optimized molecular geometries for β-CD·MeBzO-Subpc and β-CD·MePhO-Subpc inclusion complexes showed similar structural features and, therefore, the same estimated ICD signs to β-CD·BzO-Subpc (primary face: positive ICD, secondary face: negative ICD) and β-CD·PhO-Subpc (primary face: negative ICD, secondary face: negative ICD), respectively (see Figure S4 in the Supporting Information).

The widths of $(Me)_2$BzO- and $(Me)_2$PhO- substituents have been estimated to be about 6.3 Å, which is larger than the inner diameter of β-CD at the primary face (6.0 Å). Actually, the computed structures confirmed that the $(Me)_2$PhO and $(Me)_2$BzO moieties can not enter from the primary face side, whereas it is possible to form the inclusion complex with the secondary face, yielding a negative ICD signal for the Q band (Figure S4 in the Supporting Information). A comparison of the estimated ICD signals and the experimental one revealed that $(Me)_2$BzO-Subpc and $(Me)_2$PhO-Subpc can form "lid-type" inclusion complexes at the secondary face of β-CD in DMSO, but cannot form any inclusion complex with the primary face of β-CD adsorbed at the toluene/water interface.

The structure with two β-CD molecules, which was computed on the basis of the observed 2:1 composition for the β-CD·AnO-Subpc inclusion complex, is shown in Figure 10. The anthracene moiety is axially covered by the cavity of two β-CD molecules and is fully embedded, whereas the Subpc skeleton is located far from the C_7 axis of the β-CD molecule. This configuration seems reasonable because the estimated ICD signal, which shows a negative sign at the only ^1L_a band, is in good agreement with that observed in DMSO.

Conclusion

This study discovered the first example of the site-inversed formation mechanisms of the inclusion complex of CD in a bulk solution and at the liquid/liquid interface. Measurement of the interfacial tension confirmed that β-CD was adsorbed from the aqueous phase to the toluene/water inter-

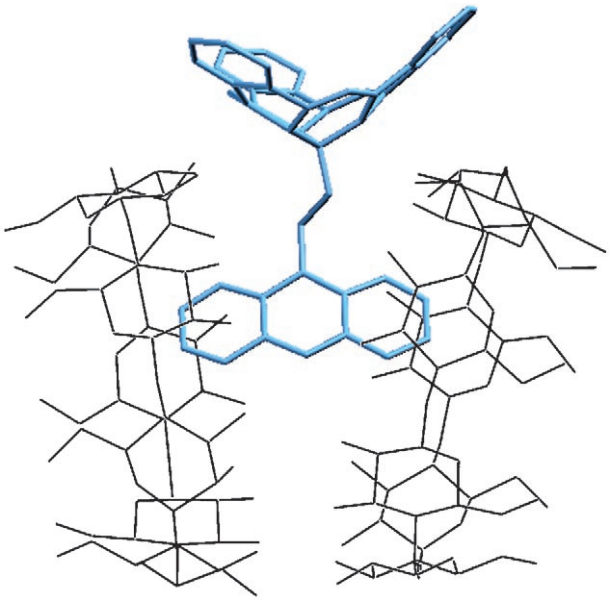

Figure 10. Estimated energy-minimized structure of the complex with a 2:1 stoichiometry between β-CD and AnO-Subpc. Hydrogen atoms are omitted for clarity.

face following the Langmuir isotherm, where the primary face was probably orientated toward the toluene phase. The stoichiometry and stability of the inclusion complex between β-CD and RO-Subpc in DMSO and at the toluene/water interface have been analyzed by CLM-CD, the high-speed stirring technique, and molecular modeling calculations. The molar ratio of the β-CD·RO-Subpc inclusion complex in DMSO was 1:1, except for AnO-Subpc (β-CD:AnO-Subpc = 2:1). On the other hand, at the toluene/water interface, β-CD formed a 1:1 inclusion complex with only four subphthalocyanines, namely BzO-Subpc, PhO-Subpc, MeBzO-Subpc, and MePhO-Subpc. The structural information from the computed modeling and the estimated sign of the ICD signals on the basis of the Tinoco–Kirkwood theory could explain the inversion of the ICD sign observed for the complexation of β-CD with BzO-Subpc and MeBzO-Subpc in DMSO and at the toluene/water interface, where the axial substitutes were accommodated by the secondary face of β-CD in DMSO and by the primary face at the toluene/water interface. In all RO-Subpc systems, the interfacial stability constants in the toluene/water system were ≈30× larger than those in DMSO. The enhancement of the stability of the inclusion complex at the toluene/water interface may be ascribed to the co-inclusion of a toluene molecule in β-CD. Scheme 3 illustrates a probable formation model of β-CD·RO-Subpc inclusion complexes suggested by the present study.

On the basis of the present study, we propose a novel concept of the chirality control of molecules bound by CD at the liquid–liquid interface, which should be very useful in various fields, such as interfacial asymmetric synthesis, molecular recognition, and chiral discrimination chemistry.

Experimental Section

Unless otherwise specified, all measurements in this study were carried out with a fixed ionic strength of 0.1 M (1 M = 1 mol dm^{-3}, sodium sulfate) at pH 6.0, adjusted with acetic acid/sodium acetate buffer, in a thermostated room at 25±2 °C.

Materials: Chloroform, 1-chloronaphthalene, diethyl ether, dimethyl sulfoxide (DMSO), and toluene, purchased from Wako Pure Chem. Co. Ltd. (Japan), were used as received, except for chloroform and toluene. Chloroform was shaken three times with 2 M (1 M = 1 mol dm^{-3}) potassium hydroxide solution, followed by shaking 3× with water, dried over calcium chloride, and then fractionally distilled. Toluene was purified according to the reported method,[65] and then saturated with distilled water prior to measuring the interfacial tension and the centrifugal liquid membrane-circular dichroism (CLM-CD). β-Cyclodextrin, which was obtained from Wako Pure Chem. Co. Ltd. (Japan), was recrystallized twice from hot water. Other chemicals (reagent grade) were obtained from Nacalai Tesque Inc., (Japan), Tokyo Kasei Kogyo Co., Ltd (Japan), or Aldrich (USA), and were used as received without further purification. The

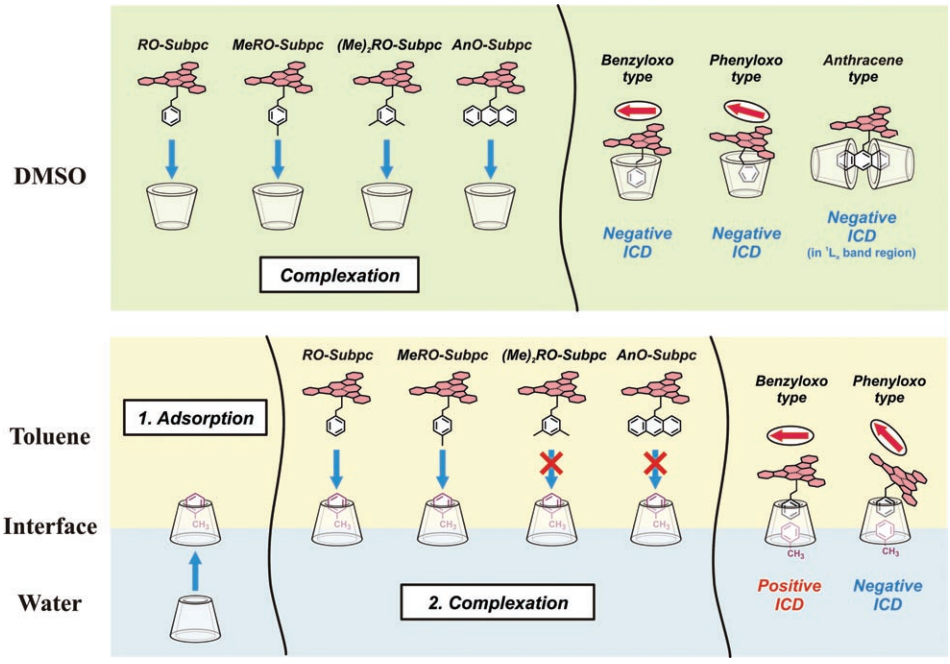

Scheme 3. Schematic illustrations of the possible conformations of β-CD·RO-Subpc inclusion complexes in DMSO (top) and at the toluene/water interface (bottom). Trapezoids represent β-CD molecules (the shorter and longer sides refer to the primary and secondary faces, respectively). The red arrows indicate the direction of the transition dipole of Subpc skeleton.

water used to prepare all samples was first distilled and then passed through a Milli-Q system (Millipore, USA) to give a specific resistivity of 18.2 MΩ cm.

General procedure for the preparation of axially substituted subphthalocyanine (RO-Subpc): The precursor chloro-[subphthalocyaninato]boron(III) (Cl-Subpc) was prepared according to published procedures.[23,24,29,30,33,66] Axially substituted subphthalocyanine was prepared by a modified procedure described in the literature.[29,33,66] A mixture of the appropriate alcohol (1.5 equiv) and Cl-Subpc (1.0 equiv) in dry toluene was heated at reflux and stirred vigorously under a nitrogen atmosphere for over 24 h. The mixture was allowed to cool and was then evaporated to dryness under reduced pressure. The residue was partitioned between water and chloroform and the aqueous layer extracted with chloroform (3×). The combined organic layers were then dried and evaporated to dryness. The crude product was purified as outlined in the following.

9-Anthracenemethyloxo[subphthalocyaninato]boron(III) (AnO-Subpc): This was prepared from 9-anthracenemethanol and Cl-Subpc and purified by column chromatography (silica gel, gradient of chloroform to 9:1 chloroform/methanol. The product was then recrystallized in methanol by adding a minimum amount of acetone to give AnO-Subpc as a reddish-purple solid. Yield: 25.38% with respect to Cl-Subpc; m.p. >250°C; TLC: R_f = 0.26 (chloroform); ^{1}H NMR (300 MHz, $CDCl_3$, 298 K): δ = 5.43 (s, 2H; O-CH_2-An), 7.45 (dd, 2H; H(2)), 7.56 (dd, 2H; H(3)), 7.86 (dd, 6H; Ar), 8.00 (d, 2H; H(4)), 8.37 (d, 2H; H(1)), 8.43 (s, 1H; H(5)), 8.80 ppm (dd, 6H; Ar); FT-IR (KBr): $\tilde{\nu}$ = 3207, 3051, 2907, 2853, 1773, 1749, 1445, 1376(B-O), 1307, 1051, 978, 884, 732, 716, 649, 604 cm^{-1}; UV/Vis (toluene): λ ($\log\varepsilon$[M^{-1}cm^{-1}])= 564 (4.84), 522 (sh), 366 (4.01), 308 (4.52) nm; MALDI-TOF/MS: *m/z*: 602 $[M]^+$, 395 $[M-\text{AnO}]^+$ [matrix: α-cyano-4-hydroxycinnamic acid (α-CHCA)]; elemental analysis calcd (%) for $C_{39}H_{23}BN_6O$: C 77.75, H 3.85, N 13.95; found: C 78.13, H 4.04, N 13.57.

Benzyloxo[subphthalocyaninato]boron(III) (BzO-Subpc): This was prepared from benzyl alcohol and Cl-Subpc, and purified by column chromatography (silica gel, chloroform). The product was then recrystallized in methanol by adding a minimum amount of diethyl ether to give BzO-Subpc as a solid with a golden luster. Yield: 79.31% with respect to Cl-Subpc; m.p. >250°C; TLC: R_f = 0.21 (chloroform); ^{1}H NMR (300 MHz, $CDCl_3$, 298 K): δ = 2.62 (s, 2H; O-CH_2-Ph), 6.39 (dd, 2H; H(1)), 6.89 (dd, 2H; H(2)), 6.91 (dd, 1H; H(3)), 7.88 (dd, 6H; Ar), 8.82 ppm (dd, 6H; Ar); FT-IR (KBr): $\tilde{\nu}$ = 3059, 2922, 2856, 1615, 1455, 1430, 1375 (B–O), 1288, 1195, 1157, 1131, 1105, 732, 697 cm^{-1}; UV/Vis (toluene): λ ($\log\varepsilon$[M^{-1}cm^{-1}])=561 (4.85), 519 (sh), 305 (4.50) nm; MALDI-TOF/MS: *m/z*: 502 $[M]^+$, 395 $[M-\text{BzO}]^+$ [matrix : α-cyano-4-hydroxycinnamic acid (α-CHCA)]; elemental analysis calcd (%) for $C_{31}H_{19}BN_6O$: C 74.12, H 3.81, N 16.73; found: C 74.01, H 3.74, N 16.57.

Phenyloxo[subphthalocyaninato]boron(III) (PhO-Subpc): This was prepared from phenol and Cl-Subpc, and purified by column chromatography (silica gel, chloroform). The product was then recrystallized in methanol by adding a minimum amount of diethyl ether (minimum amount) to give PhO-Subpc as a solid with a golden luster. Yield: 84.01% with respect to Cl-Subpc; m.p. >250°C; TLC: R_f = 0.21 (chloroform); ^{1}H NMR (300 MHz, $CDCl_3$, 298 K): δ = 5.28 (dd, 2H; H(1)), 6.58 (dd, 1H; H(3)), 6.72 (dd, 2H; H(2)), 7.90 (dd, 6H; Ar), 8.81 ppm (dd, 6H; Ar); FT-IR (KBr): $\tilde{\nu}$ = 3059, 2928, 2856, 1594, 1491, 1459, 1430, 1373 (B–O), 1285, 1232, 1195, 1130, 1052, 768, 737, 696 cm^{-1}; UV/Vis (toluene): λ ($\log\varepsilon$ [M^{-1}cm^{-1}])=562 (4.83), 520 (sh), 304 (4.45) nm; MALDI-TOF/MS: *m/z*: 790 $[M]^+$, 395 $[M-\text{PhO}]^+$ [matrix : α-cyano-4-hydroxycinnamic acid (α-CHCA)]; elemental analysis calcd (%) for $C_{30}H_{17}BN_6O$: C 73.79, H 3.51, N 17.21; found: C 74.01, H 3.74, N 17.57. These data are consistent with literature values.[66]

3,5-Dimethylbenzyloxo[subphthalocyaninato]boron(III) ((Me)$_2$BzO-Subpc): This was prepared from 3,5-dimethylbenzyl alcohol and Cl-Subpc, and purified by column chromatography (silica gel, chloroform). The product was then recrystallized into *n*-pentane from diethyl ether (minimum amount) to give (Me)$_2$PhO-Subpc as a solid with a golden luster. Yield: 82.52% with respect to Cl-Subpc; m.p. >250°C; TLC: R_f = 0.28 (chloroform); ^{1}H NMR (300 MHz, $CDCl_3$, 298 K): δ = 1.92 (s, 6H; CH_3), 2.46 (s, 2H; O-CH_2-Ph), 5.91 (s, 2H; H(1)), 6.43 (s, 1H; H(2)), 7.80 (dd, 6H; Ar), 8.75 ppm (dd, 6H; Ar); FT-IR (KBr): $\tilde{\nu}$ = 3062, 2907, 2856, 1613, 1489, 1456, 1429, 1375 (B–O), 1285, 1232, 1194, 1173, 1159, 1132, 1105, 762, 740, 697 cm^{-1}; UV/Vis (toluene): λ ($\log\varepsilon$ [M^{-1}cm^{-1}])=561 (4.87), 520 (sh), 306 (4.49) nm; MALDI-TOF/MS: *m/z*: 530 $[M]^+$, 395 $[M-(\text{Me})_2\text{BzO})]^+$ [matrix : α-cyano-4-hydroxycinnamic acid (α-CHCA)]; elemental analysis calcd (%) for $C_{33}H_{23}BN_6O$: C 74.73, H 4.37, N 15.85; found: C 75.25, H 4.74, N 15.57.

3,5-Dimethylphenyloxo[subphthalocyaninato]boron(III) ((Me)$_2$PhO-Subpc): This was prepared from 3,5-dimethylphenol and Cl-Subpc, and purified by column chromatography (silica gel, chloroform). The product was then recrystallized into *n*-pentane from diethyl ether (minimum amount) to give MePhO-Subpc as a solid with a golden luster. Yield: 78.55% with respect to Cl-Subpc; m.p. >250°C; TLC: R_f = 0.29 (chloroform); ^{1}H NMR (300 MHz, $CDCl_3$, 298 K): δ = 1.95 (s, 6H; CH_3), 5.15 (s, 2H; H(1)), 6.59 (s, 1H; H(3)), 7.81 (dd, 6H; Ar), 8.78 ppm (dd, 6H; Ar); FT-IR (KBr): $\tilde{\nu}$ = 3055, 2812, 1614, 1489, 1455, 1430, 1367(B-O), 1287, 1230, 1194, 1171, 1157, 1130, 1104, 731, 695 cm^{-1}; UV/Vis (toluene): λ ($\log\varepsilon$[M^{-1}cm^{-1}])=563 (4.87), 520 (sh), 305 (4.47) nm; MALDI-TOF/MS: *m/z*: 516 $[M]^+$, 395 $[M-(\text{Me})_2\text{BzO}]^+$] [matrix : α-cyano-4-hydroxycinnamic acid (α-CHCA)]; elemental analysis calcd (%) for $C_{32}H_{21}BN_6O$: C 74.43, H 4.10, N 16.28; found: C 74.75, H 4.34, N 16.25.

4-Methylbenzyloxo[subphthalocyaninato]boron(III) (MeBzO-Subpc): This was prepared from 4-methylbenzyl alcohol and Cl-Subpc, and purified by column chromatography (silica gel, chloroform). The product was then recrystallized into methanol from diethyl ether (minimum amount) to give MePhO-Subpc as a as a solid with a golden luster. Yield: 84.03% with respect to Cl-Subpc; m.p. >250°C; TLC: R_f = 0.24 (chloroform); ^{1}H NMR (300 MHz, $CDCl_3$, 298 K): δ = 2.06 (s, 3H; CH_3), 2.57 (s, 2H; O-CH_2-Ph), 6.26 (d, 2H; H(1)), 6.70 (d, 2H; H(2)), 7.86 (dd, 6H; Ar), 8.80 ppm (dd, 6H; Ar); FT-IR (KBr): $\tilde{\nu}$ = 3056, 2908, 1614, 1456, 1429, 1369(B-O), 1348, 1286, 1229, 1193, 1174, 1158, 1131, 1110, 761, 737, 696 cm^{-1}; UV/Vis (toluene): λ ($\log\varepsilon$[M^{-1}cm^{-1}])= 562 (4.84), 519 (sh), 306 (4.50) nm; MALDI-TOF/MS: *m/z*: 516 $[M]^+$, 395 $[M-\text{PhO}]^+$ [matrix : α-cyano-4-hydroxycinnamic acid (α-CHCA)]; elemental analysis calcd (%) for $C_{33}H_{23}BN_6O$: C 74.73, H 4.37, N 15.85; found: C 75.44, H 4.44, N 16.07.

4-Methylphenyloxo[subphthalocyaninato]boron(III) (MePhO-Subpc): This was prepared from 4-methylphenol and Cl-Subpc, and purified by column chromatography (silica gel, chloroform). The product was then recrystallized into methanol from diethyl ether (minimum amount) to give MePhO-Subpc as a as a solid with a golden luster. Yield: 79.31% with respect to Cl-Subpc; mp >250°C; TLC: R_f = 0.27 (chloroform); ^{1}H NMR (300 MHz, $CDCl_3$, 298 K): δ = 2.04 (s, 3H; CH_3), 5.15 (d, 2H; H(1)), 6.51 (d, 2H; H(2)), 7.88 (dd, 6H; Ar), 8.82 (dd, 6H; Ar); FT-IR (KBr): $\tilde{\nu}$ = 3053, 2972, 1509, 1457, 1431, 1366 (B–O), 1348, 1285, 1234, 1194, 1168, 1129, 1079, 1056, 765, 742, 692 cm^{-1}; UV/Vis (toluene): λ ($\log\varepsilon$[M^{-1}cm^{-1}])= 563 (4.83), 521 (sh), 302 (4.49) nm; MALDI-TOF/MS: *m/z*: 502 $[M]^+$, 395 $[M-\text{MePhO}]^+$ [matrix : α-cyano-4-hydroxycinnamic acid (α-CHCA)]; elemental analysis calcd (%) for $C_{31}H_{19}BN_6O$: C 74.12, H 3.81, N 16.73; found: C 74.09, H 3.84, N 16.47.

Centrifugal liquid membrane-circular dichroism (CLM-CD) spectroscopy: Circular dichroism measurements of interfacial β-CD complexes were performed on a spectropolarimeter (J-810E, JASCO, Japan) equipped with a centrifugal liquid-membrane (CLM) cell in its sample chamber.[52] The apparatus for the CLM-CD measurement was essentially the same as that previously reported.[53] A cylindrical cell, whose height and outer diameter were 3.3 and 2.1 cm, respectively, was placed horizontally in the sample chamber and rotated at 10000 rpm by a speed-controlled electric motor (NE-22E, Nakanishi Inc., Japan). The sample chamber was flushed with a constant stream of dry air to avoid an increase in temperature by the electric motor of the CLM apparatus. The toluene solution of RO-Subpc and the aqueous solution of β-CD (each 0.500 mL) were introduced into the cylindrical cell by means of a microsyringe. The sum of the CD spectra of the bulk phases and the interface was measured in the range of 300–650 nm. The aqueous and toluene phases with RO-Subpc, but without β-CD, in the CLM cell was used for a baseline measurement.

Interfacial tension measurement: The interfacial tension, γ, of a β-CD monolayer at the toluene/water interface was measured by Wilhelmy balance technique with a 10.0×10.0 mm filter paper plate (Hybrid Instruments Co., Japan). Into a glass sample tube ($\varphi = 30$ mm), treated with dichlorodimethylsilane for hydrophobic coating so as to make a flat toluene/water interface and thermostatted with a water jacket at 25 ± 0.1 °C were added water (25 mL) and then toluene (25 mL). A measured small volume of an aqueous solution of β-CD was added into the aqueous phase with a microsyringe. This procedure was repeated to produce an incremental increase in the concentration of β-CD. It took at least 1 h before the interfacial tension reached equilibrium. The interfacial tension was measured with a precision of ±0.05 mN m^{-1}.

Batch experiments: An aliquot (10 mL) of the aqueous solution containing 1.0×10^{-4} M β-CD was transferred into a 50-mL cylindrical glass tube with a stopper. After the addition of 1.0×10^{-5} M RO-Subpc in toluene (10 mL), the mixture was agitated for 60 min at 200 reciprocation min^{-1} in a thermostated incubator (LT-10F SX, Taitec Corp., Japan) at 25 ± 0.1 °C. After the mixture was centrifuged at 2000 rpm for 5 min, the CD spectra of the separated toluene and aqueous phases were measured.

High-speed stirring (HSS) method: The interfacial stability constant of the β-CD·RO-Subpc inclusion complex was measured by means of the high-speed stirring (HSS) technique.[55] The toluene phase (50 mL), containing the dissolved RO-Subpc compounds, and the aqueous phase (50 mL), containing the β-CD, were vigorously agitated in a glass stirring cell thermostatted with a water jacket at 25 ± 0.1 °C at 5000 rpm (high-speed stirring) by an electric motor (Nikko Keisoku SC-5, Japan), to generate a large interfacial area. After a few min, the speed was reduced to 200 rpm (low-speed stirring), to properly separate the two phases. The bulk toluene phase was continuously separated from the agitated mixture by a PTFE phase separator and circulated through a flow cell with an optical pathlength of 10 mm at a flow rate of $\approx$20 mL min^{-1}. The absorption spectra of the toluene phase were continuously measured in the range $\lambda = 300$–650 nm with a photodiode-array UV/Vis detector (SPD-M^{6}A, Shimadzu, Japan). The quantity of interfacial β-CD·RO-Subpc inclusion complex was calculated from the difference between the absorbances at both stirring speeds.

Other apparatus: Melting points were determined on a MP-500D melting point apparatus (Yanako, Japan) and were uncorrected. Column chromatography was performed with Wakogel C-200 (silica-gel, Wako, Japan). ^{1}H NMR spectra were recorded on a Unity 300 spectrometer (Varian, USA). Chemical shifts of ^{1}H NMR spectra are relative to an internal standard of TMS. Elemental analyses were carried out with a CHNS/O analyzer 2400 (Perkin-Elmer, USA). IR spectra (KBr disk) were measured with a MAGNA-IR 560 FT-IR spectrometer (Nicolet, USA). MALDI-TOF mass spectra were obtained on a Voyager DE-Pro spectrometer (PerSeptive Biosystems, UK) with α-cyano-4-hydroxycinnamic acid (α-CHCA) as a matrix. The pH of the aqueous phase was measured with a F-14 pH meter (HORIBA, Japan) equipped with a 6366-10D glass electrode. UV/Vis and CD spectra were recorded on a V-570 spectrometer (JASCO, Japan) and J-810 spectropolarimeter (JASCO, Japan), respectively.

Estimation of the induced circular dichroism spectra: Harata et al.[67,68] used the Tinoco–Kirkwood equation[31,32] in a form that was suitable for the calculation of the rotatory strength, R_{0a}, of CD inclusion complexes in the j-th transition from the ground state, 0, to an excited state, a [Eq. (12)]:

$$R_{0a} = \pi\nu_a\mu_{0a}^2\sum_j \frac{\nu_{0j}^2(\alpha_{33}-\alpha_{11})_j(\mathrm{GF})_j}{c(\nu_{0j}^2-\nu_a^2)} \qquad (12)$$

where α_{11} and α_{33} represent bond polarizabilities at zero frequency, parallel and perpendicular to the symmetry axis of the j-th bond, respectively, c is the velocity of light, and ν_{0j} and ν_a are frequencies of the electric transitions of host and guest, respectively, that are located at a distance r_j. The geometrical factor, $(\mathrm{GF})_j$, is defined in Equation (13):

$$(\mathrm{GF})_j = \frac{1}{r_j^3}\left\{e_{0a}e_j-\frac{3(e_{0a}r_j)(e_jr_j)}{r_j^2}\right\}e_{0a}e_jr_j \qquad (13)$$

where, e_{0a} and e_j are unit vectors along the electric transition moment μ_{0a} and parallel to the j–th bond, respectively. The origin of the system was located in the center of β-CD molecule, while the z axis was the C_7 axis as shown in Scheme 1. The geometry of β-CD was determined from the X-ray crystal data obtained from the Cambridge Crystallographic Database. In accordance with the procedure recommended by Kodama et al.,[69] all the C6–O6 and O–H bonds were neglected owing to their flexibility, and all C–H bonds were also neglected because they may have isotropic polarizability. The averaged frequencies of the electric transitions, ν_{0j}, and polarizability, α, of the bonds in a glucose residue were, respectively, ν_{0j}: 70850 cm^{-1} for (C–C) and 67530 cm^{-1} for (C–O)), and $\alpha_{33}-\alpha_{11;}$ 0.71 Å^3 for (C–C) and 0.43 Å^3 for (C–O).

Molecular modeling: All molecular modeling calculations were carried out on a DELL Pentium4 3.2 GHz personal computer operating under Windows XP SP2. The MM2 force field[70] and the semiempirical PM3 method[71] implemented in HyperChem[72] were used. The geometry parameters of β-CD were taken from X-ray diffraction data in the Cambridge Crystallographic Database. The structure of the RO-Subpc compounds were built with HyperChem, and its geometry was then minimized to attain the energy gradient of 0.1 kcal Å^{-1} mol with the MM2 force field with the Polak–Ribiere (conjugate gradient) minimizer. The results were used as initial structures for semiempirical SCF-MO calculations with the PM3 Hamiltonian. The geometry optimization was carried out by with the Polak–Ribiere algorithm to a maximum energy gradient of 0.05 kcal Å^{-1} mol. The calculations were conducted as if the system was in a vacuum. The conformation of β-CD/RO-Subpc complexes were built by docking the structure of RO-Subpc compounds into the cavity of β-CD and then minimizing the energy of the complex with molecular mechanics.[73,74]

Acknowledgements

This study was supported by the Grant-in-Aid for Scientific Research (S) (No. 16105002) of the Ministry of Education, Culture, Sports, Science and Technology of Japan. K.A. is PhD student supported by the MORESCO contact education program.

[1] M. L. Bender, M. Komiyama, *Cyclodextrin Chemistry: Reactivity and Structure, Concepts in Organic Chemistry*, Springer, New York, USA, **1978**.
[2] J. Szejtli, *Cyclodextrin Technology (Topics in Inclusion Science)*, Kluwer, Dordrecht, **1988**.
[3] *Cyclodextrin: Fundamentals and Applications* (Eds.: F. Toda, A. Ueno), Sangyo-Tosho, Tokyo, **1995**.
[4] B. Feibush, C. L. Woolley, V. Mani, *Anal. Chem.* **1993**, *65*, 1130–1133.
[5] A. Nakamura, Y. Inoue, *J. Am. Chem. Soc.* **2003**, *125*, 966–972.
[6] H. Aoyama, K. Miyazaki, M. Sakamoto, Y. Omote, *Tetrahedron* **1987**, *43*, 1513–1518.
[7] T. Tamaki, T. Kokubu, K. Ichimura, *Tetrahedron* **1987**, *43*, 1485–1494.
[8] H. Takeshita, M. Kumamoto, I. Kouno, *Bull. Chem. Soc. Jpn.* **1980**, *53*, 1006–1009.
[9] M. Miyauchi, A. Harada, *J. Am. Chem. Soc.* **2004**, *126*, 11418–11419.
[10] N. Ueyama, A. Harada, *Macromolecular Nanostructured Materials (Springer Series in Materials Science)*, Springer, New York, **2005**.
[11] S. Sasaki, Y. Takase, K. Koga, *Tetrahedron Lett.* **1990**, *31*, 6051–6054.
[12] J. I. Seeman, H. V. Secor, D. W. Armstrong, K. D. Timmons, T. J. Ward, *Anal. Chem.* **1998**, *70*, 2120–2127.
[13] J. Hamilton, L. Chen, *J. Am. Chem. Soc.* **1988**, *110*, 5833–5841.

[14] S. D. P. Baugh, Z. Yang, D. K. Leung, D. M. Wilson, R. Breslow, *J. Am. Chem. Soc.* **2001**, *123*, 12488–12494.
[15] H. H. Sigurdsson, E. Knudsen, T. Loftsson, N. Leeves, J. F. Sigurjonsdottir, M. Másson, *J. Inclusion Phenom. Macrocyclic Chem.* **2002**, *44*, 169–172.
[16] V. J. Stella, V. M. Rao, E. A. Zannou, V. Zia, *Adv. Drug Delivery Rev.* **1999**, *36*, 3–16.
[17] H. Watarai, S. Tsukahara, H. Nagatani, A. Ohashi, *Bull. Chem. Soc. Jpn.* **2003**, *76*, 1471–1492.
[18] *Liquid Interfaces in Chemical, Biogical and Pharmaceutical Appreciations* (Ed.: A. G. Volkov), Marcel Dekker, New York, USA, **1997**.
[19] C. Z. Huang, Y. H. Wang, H. P. Guo, Y. F. Li, *Analyst* **2005**, *130*, 200–205.
[20] Y. Yulizar, H. Monjushiro, H. Watarai, *J. Colloid Interface Sci.* **2004**, *275*, 560–569.
[21] K. Fujiwara, H. Monjushiro, H. Watarai, *Chem. Phys. Lett.* **2004**, *394*, 349–353.
[22] H. Ringsdorf, B. Schlarb, J. Venzmer, *Angew. Chem.* **1988**, *100*, 117–162; *Angew. Chem. Int. Ed. Engl.* **1988**, *27*, 113–158.
[23] A. Meller, A. Ossko, *Monatsh. Chem.* **1972**, *103*, 150–155.
[24] C. G. Claessens, D. González-Rodríguez, T. Torres, *Chem. Rev.* **2002**, *102*, 835–853.
[25] N. Kobayashi, R. Kondo, S. Nakajima, T. Os, *J. Am. Chem. Soc.* **1990**, *112*, 9640–9641.
[26] H. Eichhorn, D. Wöhrle, D. Pressner, *Liq. Cryst.* **1997**, *22*, 643–653.
[27] S. H. Kang, K. Kim, Y.-S. Kang, W. C. Zin, G. Olbrechts, K. Wostyn, K. Clays, A. Persoons, *Chem. Commun.* **1999**, 1661–1662.
[28] M. A. Díaz-García, F. Agulló-López, A. Sastre, T. Torres, W. E. Torruellas, G. I. Stegeman, *J. Phys. Chem.* **1995**, *99*, 14988–14991.
[29] G. de la Torre, P. Vázquez, F. Agulló-López, T. Torres, *Chem. Rev.* **2004**, *104*, 3723–3750.
[30] C. G. Claessens, D. González-Rodríguez, T. Torres, G. Martín, F. Agulló-López, I. Ledoux, J. Zyss, V. R. Ferro, J. M. García de la Vega, *J. Phys. Chem. B* **2005**, *109*, 3800–3806.
[31] I. Tinoco, Jr., *Adv. Chem. Phys.* **1962**, *4*, 113–160.
[32] J. G. Kirkwood, *J. Chem. Phys.* **1937**, *5*, 479–491.
[33] C. G. Claessens, D. G. Rodríguez, B. del Rey, T. Torres, G. Mark, H.-P. Schuchmann, C. von Sonntag, J. G. MacDonald, R. S. Nohr, *Eur. J. Org. Chem.* **2003**, 2547–2551.
[34] R. L. Werner, K. G. O'Brien, *Aust. J. Chem.* **1955**, *8*, 355–360.
[35] S. Suzuki, T. Fujii, H. Baba, *J. Mol. Spectrosc.* **1973**, *47*, 243–251.
[36] N. Kobayashi, T. Ishizaki, K. Ishii, H. Konami, *J. Am. Chem. Soc.* **1999**, *121*, 9096–9110.
[37] D. J. Wood, F. E. Hruska, W. Saenger, *J. Am. Chem. Soc.* **1977**, *99*, 1735–1740.
[38] N. Kobayashi, T. Osa, *Carbohydr. Res.* **1989**, *192*, 147–157.
[39] R. L. VanEtten, J. F. Sebastian, G. A. Clowes, M. L. Bender, *J. Am. Chem. Soc.* **1967**, *89*, 3242–3253.
[40] R. L. VanEtten, G. A. Clowes, J. F. Sebastian, M. L. Bender, *J. Am. Chem. Soc.* **1967**, *89*, 3253–3262.
[41] T. S. Straub, M. L. Bender, *J. Am. Chem. Soc.* **1972**, *94*, 8875–8881.
[42] T. S. Straub, M. L. Bender, *J. Am. Chem. Soc.* **1972**, *94*, 8881–8888.
[43] S. Hamai, *Bull. Chem. Soc. Jpn.* **1982**, *55*, 2721–2729.
[44] M. Ma, D. Li, *Chem. Mater.* **1999**, *11*, 872–874.
[45] H. Zhou, J. T. Groves, *J. Porphyrins Phthalocyanines* **2004**, *8*, 125–140.
[46] H. A. Benesi, J. H. Hildebrand, *J. Am. Chem. Soc.* **1949**, *71*, 2703–2707.
[47] I. Sanemasa, Y. Akamine, *Bull. Chem. Soc. Jpn.* **1987**, *60*, 2059–2066.
[48] I. Langmuir, *J. Am. Chem. Soc.* **1917**, *39*, 1848–1906.
[49] H. Watarai, F. Funaki, *Langmuir* **1996**, *12*, 6717–6720.
[50] G. Marconi, B. Mayer, *Pure Appl. Chem.* **1997**, *69*, 779–783.
[51] B. Mayer, G. Marconi, C. Klein, G. Köhlerl, P. Wolschann, *J. Inclusion Phenom. Mol. Recognit. Chem.* **1997**, *29*, 79–93.
[52] S. Wada, H. Monjushiro, H. Watarai, *Anal. Sci.* **2004**, *20*, 1489–1491.
[53] H. Nagatani, H. Watarai, *Anal. Chem.* **1998**, *70*, 2860–2865.
[54] P. Job, *Ann. Chim. Phys.* **1928**, *9*, 113–203.
[55] H. Watarai, K. Sasaki, K. Takahashi, J. Murakami, *Talanta* **1995**, *42*, 1691–1700.
[56] H. Watarai, M. Gotoh, N. Gotoh, *Bull. Chem. Soc. Jpn.* **1997**, *70*, 957–964.
[57] Y. Liu, Y. Zhao, E. Yang, H. Zhang, *J. Inclusion Phenom. Macrocyclic Chem.* **2004**, *50*, 3–11.
[58] D. Krois, U. H. Brinker, *J. Am. Chem. Soc.* **1998**, *120*, 11627–11632.
[59] G. Grabner, S. Monti, G. Marconi, B. Mayer, C. Klein, G. Köhler, *J. Phys. Chem.* **1996**, *100*, 20068–20075.
[60] R. S. Murphy, T. C. Barros, B. Mayer, G. Marconi, C. Bohne, *Langmuir* **2000**, *16*, 8780–8788.
[61] B. Mayer, X. Zhang, W. M. Nau, G. Marconi, *J. Am. Chem. Soc.* **2001**, *123*, 5240–5248.
[62] H. Bakirci, X. Zhang, W. M. Nau, *J. Org. Chem.* **2005**, *70*, 39–46.
[63] G. Martín, G. Rojo, F. Agulló-López, V. R. Ferro, J. M. G. Vega, M. V. Martínez-Díaz, T. Torres, I. Ledoux, J. Zyss, *J. Phys. Chem. B* **2002**, *106*, 13139–13145.
[64] N. Kobayashi, *J. Chem. Soc. Chem. Commun.* **1988**, 918–919.
[65] J. A. Riddick, W. B. Bunger, T. K. Sakano, *Organic Solvents* (4th ed.), Wiley, New York, USA, **1986**.
[66] K. Kasuga, T. Idehara, M. Handa, Y. Ueda, T. Fujiwara, K. Isa, *Bull. Chem. Soc. Jpn.* **1996**, *69*, 2559–2563.
[67] K. Harata, H. Uedaira, *Bull. Chem. Soc. Jpn.* **1975**, *48*, 375–378.
[68] K. Harata, *Bull. Chem. Soc. Jpn.* **1979**, *52*, 1807–1812.
[69] M. Kodaka, T. Fukaya, *Bull. Chem. Soc. Jpn.* **1989**, *62*, 1154–1157.
[70] N. L. Allinger, *J. Am. Chem. Soc.* **1977**, *99*, 8127–8134.
[71] J. J. P. Stewart, *J. Comput. Chem.* **1989**, *10*, 221–264.
[72] Hyperchem 6.0 for Windows; Hypercube, Inc., **2000**.
[73] F. Pérez, C. Jaime, X. Sanchez-Ruiz, *J. Org. Chem.* **1995**, *60*, 3840–3845.
[74] P. E. Schipper, A. Rodger, *J. Am. Chem. Soc.* **1983**, *105*, 4541–4550.

Received: October 26, 2005
Revised: January 13, 2006
Published online: March 31, 2006

